Iodine Retention of Long-chain Organic Iodides on Silver-based Sorbents under DOG and VOG Conditions

Nuclear Technology Research and Development

Approved for public release. Distribution is unlimited.

Prepared for
U.S. Department of Energy
Material Recovery and Waste Form Development Campaign

S. H. Bruffey, A. T. Greaney,
R. T. Jubin (ORNL)
N. R. Soelberg, A. Welty (INL)

Oak Ridge National Laboratory
Idaho National Laboratory
30 September 2019
ORNL/SPR-2019/1359
INL/EXT-19-55999

SUMMARY

The aqueous reprocessing of used nuclear fuel releases four key volatile radionuclides (^{3}H, ^{14}C, ^{85}Kr, and ^{129}I) from the used fuel into the off-gas streams of a reprocessing facility. Some semi-volatile radionuclides such as ^{106}Ru may also be released into the gas streams. Compliance with US regulations may require removal of these radionuclides from the off-gas streams before their discharge to the environment (Jubin et al. 2017). Iodine is released during multiple unit operations within a plant and can be found in gas streams such as the shear off-gas, dissolver off-gas, vessel off-gas (VOG), and waste solidification off-gas. To achieve DFs >1,000, treatment of the plant off-gas streams must include, at minimum, removal of both the dissolver off-gas and VOG.

A 2015 analysis showing that the speciation of iodine in the VOG is primarily composed of organic alkyl iodides and that abatement technology for organic iodides is not well developed has produced increased interest in removing iodine from VOG. The lack of knowledge surrounding iodine removal from the VOG prompted the Office of Nuclear Energy within the US Department of Energy to initiate experimental efforts targeted at understanding organic iodide removal from prototypic VOG streams. In 2018 a joint test plan was developed and issued by Oak Ridge National Laboratory and Idaho National Laboratory. This test plan is intended to guide a multiyear experimental effort that will provide substantial amounts of information about the removal of organic iodides from VOG streams.

This document reports on the progress of Idaho National Laboratory and Oak Ridge National Laboratory in the execution of the joint test plan as of the end of fiscal year 2019. Silver-based sorbents are the primary removal technology being characterized, and this report includes data on iodine adsorption by reduced silver-exchanged mordenite (also called silver-exchanged zeolite [AgZ]) (as a baseline iodine sorbent) and silver-functionalized silica aerogel (AgAero or Ag Aerogel) (as an advanced iodine sorbent). Conclusions are preliminary in nature and reflect the ongoing execution of the test plan through close collaboration between the two laboratories.

CONTENTS

FIGURES

TABLES

ACRONYMS

AgZ	silver-reduced silver-exchanged mordenite
AgAero	silver-functionalized silica aerogel
DF	decontamination factor
DOG	dissolver off-gas
INL	Idaho National Laboratory
MTZ	mass transfer zone
ORNL	Oak Ridge National Laboratory
UNF	used nuclear fuel
VOG	vessel off-gas
WOG	waste solidification off-gas

IODINE RETENTION OF LONG-CHAIN ORGANIC IODIDES ON SILVER-BASED SORBENTS UNDER DOG AND VOG CONDITIONS

1. INTRODUCTION

The aqueous reprocessing of used nuclear fuel (UNF) releases four key volatile radionuclides (^{3}H, ^{14}C, ^{85}Kr, and ^{129}I) from the used fuel into the off-gas streams of the reprocessing facility. Some semi-volatile radionuclides such as ^{106}Ru may also be released into the gas streams. Compliance with US regulations may require that these radionuclides be removed from the off-gas streams before their discharge to the environment (Jubin et al. 2017). These regulations are especially stringent for the release of ^{129}I, which has the longest half-life of the radionuclides listed and can have a significant biological impact. An evaluation was conducted that assessed the practical impact of these regulations. An overall plant decontamination factor (DF)[a] of 1,000 is the minimum required abatement efficiency (Jubin et al. 2012) and depending on the specifics of the reprocessing facility and reprocessed fuel, the required DF could be as high as 8,000.

Iodine is released during multiple unit operations within the plant and can be found in gas streams such as the shear off-gas, dissolver off-gas (DOG), vessel off-gas (VOG), and waste solidification off-gas (WOG). An analysis of the distribution of iodine between aqueous separations unit operations found that 95–99% of total iodine release to the off-gas occurs during dissolution (releasing the iodine into the DOG) and that much of the balance of the iodine is released during solvent extraction (releasing the iodine into the VOG) (Jubin et al. 2013). To achieve DFs >1,000, treatment of the plant off-gas streams must include at minimum, treatment of both the DOG and VOG.

Removal of iodine from the DOG has been the subject of substantial research and development in recent years. Iodine is primarily present in the DOG as elemental iodine (I_2) and is typically removed using silver-based sorbent materials or aqueous caustic scrubbing. A 2015 analysis showing that the speciation of iodine in the VOG is primarily composed of organic alkyl iodides and that abatement technology for organic iodides is not well developed has produced increased interest in removing iodine from VOG (Bruffey et al. 2015). Further, the concentration of iodine in the VOG (parts per billion [ppb] by volume levels) is substantially lower than that of the DOG (parts per million [ppm] by volume levels), and the characteristics of the two gas streams differ in total flowrate, volume, and composition.

The lack of knowledge about iodine removal from VOG prompted the Office of Nuclear Energy within the US Department of Energy to initiate experimental efforts targeted at understanding organic iodide removal from prototypic VOG streams. To date, a number of experiments have been performed at Idaho National Laboratory (INL) and Oak Ridge National Laboratory (ORNL) focused on this topic. In 2018 a joint test plan was developed and issued by the two laboratories (Jubin et al. 2018) that is intended to guide a multiyear experimental effort to provide information about the removal of organic iodides from VOG streams. The data collected are expected to eventually be used to refine engineering and full-scale iodine abatement technology for use in treating the VOG.

This document reports on INL and ORNL's progress in the execution of the joint test plan as of the end of fiscal year 2019 and characterizes silver-based sorbent removal technology. This report includes data for iodine adsorption by reduced silver-exchanged mordenite (also called silver-exchanged zeolite [AgZ]) (as

[a] Decontamination factor (DF) = $\frac{Flowrate\ of\ radionuclide\ in\ a\ control\ device\ inlet\ gas}{Flowrate\ of\ radionuclide\ in\ a\ control\ device\ outlet\ gas}$

a baseline iodine sorbent) and silver-functionalized silica aerogel (AgAero or Ag Aerogel) (as an advanced iodine sorbent).

2. JOINT TEST PLAN OBJECTIVES

The joint test plan references several key types of data that are needed to advance organic iodine removal. An engineering design requires knowledge of the mass transfer zone (MTZ) and achievable overall DF. Fundamental high-priority data includes measuring the iodine saturation capacity and rate of iodine adsorption for each organic iodide species on the selected silver-based sorbent.

As listed in the joint test plan, there are seven primary questions under investigation (Jubin et al. 2018).

1. *Is the adsorption rate a function of hydrocarbon chain length?*
2. *Is the adsorption rate a function of long-chain organic iodide concentration?*
3. *What is the effect of the gas velocity on the behavior observed in questions 1–2?*
4. *What is the saturation concentration of iodine for various long-chain organic iodides on silver-based sorbents, and does it vary with target feed species?*
5. *What is the DF over a fixed length of bed as a function of concentration and iodine species in the feed gas?*
6. *If the adsorption rate changes, which is impacted the most: the DF, bed penetration depth, or bed penetration rate? (This is the combined effect of the results of questions 1, 2, 3, and 5.)*
7. *What is the length and shape of the MTZ, and how do they vary or change for CH_3I and other organic iodides on silver-based sorbents?*

This report describes experiments relating to the first two questions of adsorption rate as a function of hydrocarbon chain length and concentration. Preliminary data also inform the answers to questions 4, 5, and 7 relating to the saturation concentration of the sorbent and the adsorption mass transfer zone. This testing was guided by conditions specified in the joint test plan and substantial additional details can be found therein.

Table 2-1 summarizes tests performed at INL and ORNL since the issuance of the joint test plan. These tests focused on iodine capture from VOG streams, recognizing that recent tests have focused more on iodine capture from DOG streams than from VOG streams. The tests are broadly categorized into thin bed testing conducted at ORNL, deep bed testing conducted at ORNL, and deep bed testing conducted at INL. The three types of tests are complementary, with each having different objectives and returning different types of data.

ORNL previously performed deep bed VOG tests at iodine concentrations as low as 7 ppb I_2; these tests are performed at concentrations orders of magnitude lower than deep bed testing at INL, which is performed at ~1 ppm iodine concentration in the feed stream (Jubin et al. 2017). INL is able to saturate the sorbent in practical time frames, determine an MTZ, and measure iodine in the effluent from the bed to determine DF. The data obtained by ORNL are the penetration depth of the sorbate into the deep bed and the maximum observed iodine loading. ORNL data allows validation of sorbent behavior at extremely low iodine concentrations, while INL data indicates potential DFs and MTZ depths.

Table 2-1. Test descriptions.

Designation	Type	Iodine species	Nominal iodine concentration	Sorbent	Water dew point (°C)	Laboratory
VOG19-2	Deep bed	C_4H_9I	1,000 ppb	AgZ	0	ORNL
FY19-010-38	Thin bed	C_4H_9I	42,000 ppb	AgZ	−70	ORNL
FY19-012-38	Thin bed	C_4H_9I	10,000 ppb	AgZ	−70	ORNL
VOG-C_4H_9I-1 AgA	Deep bed	C_4H_9I	1,000 ppb	AgAero	−60	INL
VOG-CH_3I-2 AgZ	Deep bed	CH_3I	2,000 ppb	AgZ	0	INL

As shown in Table 2-1, the tests reported here are focused primarily on the adsorption of methyl iodide (CH_3I) and iodobutane (C_4H_9I) by AgZ and AgAero. The data from these tests were synthesized with previously obtained INL and ORNL data on the adsorption of iodine from I_2, CH_3I, and C_4H_9I by AgZ and AgAero. Experimental efforts are also planned to evaluate iodine adsorption from iodododecane [$C_{12}H_{25}I$]. Those $C_{12}H_{25}I$ experiments have been delayed after initial studies at INL indicated challenges with producing a simulated gas stream containing $C_{12}H_{25}I$ (Soelberg 2017).

3. MATERIALS AND METHODS

The methods, materials, and systems used to perform iodine adsorption tests at INL and ORNL are summarized here.

3.1 INL Deep Bed Testing

The deep bed test system and test materials and methods are described in detail in Soelberg (2019). An abbreviated version is described here. This test system was first used in 2009 for iodine adsorption testing (Haefner 2009), and since then it has been used in additional iodine adsorption tests. Results of some of those tests are included in this report. The original test system has evolved, and the current test system (Figure 3-1) includes (a) a gas supply and blending system, which supplies gases from building compressed air, gas cylinders, gas generators, and a humidifier; (b) a multiple-segment sorbent bed system inside a heated oven; and (c) an inlet and bed segment outlet gas sampling system. Iodide gases including diatomic iodine and organic iodides are produced using a VICI Metronics Dynacalibrator Model 190 gas generator system that contains calibrated gas permeation tubes. The iodine-bearing gas is then blended with other gases at flowrates that simulate the target DOG, VOG, or other gas stream compositions. This gas stream is passed through a multiple sorbent deep bed system inside a heated oven.

This test system has the capability to sample and analyze the gas flow at the inlet and after each bed segment and to sample and analyze the sorbent from any selected bed segment at selected test durations. Gas analysis is performed by gas chromatography (gas chromatography with flame ionization detection) or gas scrubbing followed by analysis using inductively coupled plasma mass spectroscopy. Solids can be analyzed using wet chemistry methods or scanning electron microscope–energy dispersive spectroscopy.

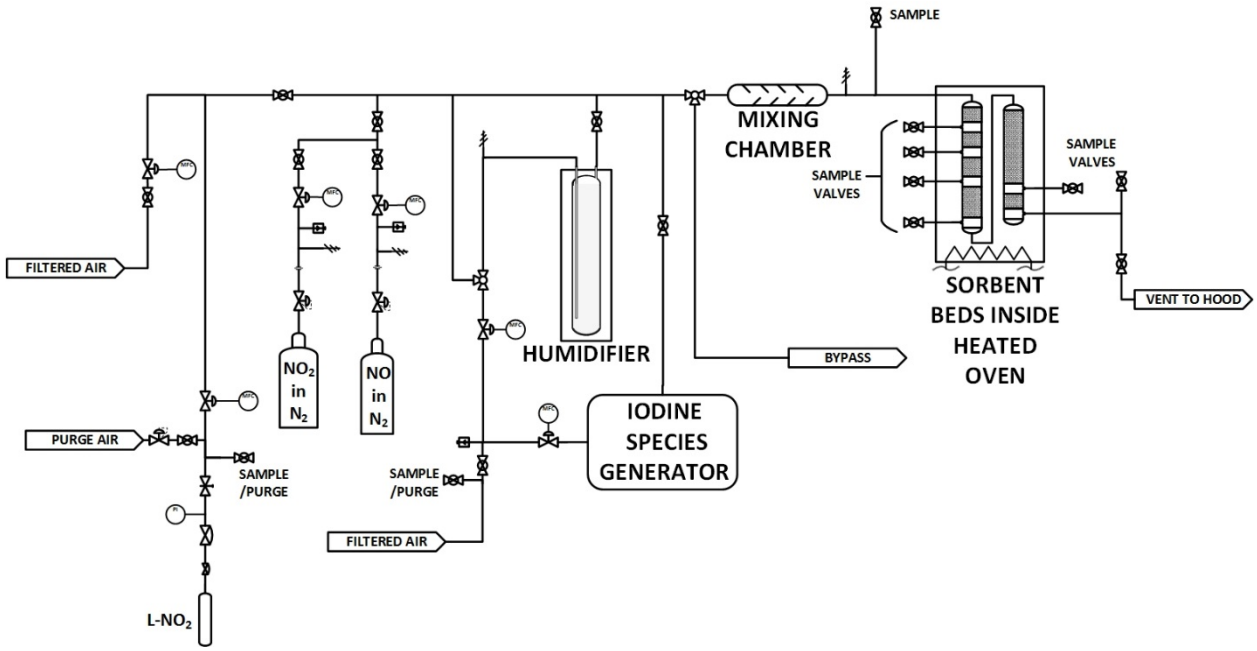

Figure 3-1. INL deep bed test system.

Figures 3-2 and 3-3 show detail of the sorbent beds and how the sorbent beds are configured in a temperature-controlled oven. The current INL test design can include at least six sorbent bed segments. The sorbent bed segments are made of borosilicate glass with a glass frit at the bottom of each bed segment to support the granular sorbent. The gas flows downward through the beds to prevent any agitation of the bed particles in the event of high gas flows.

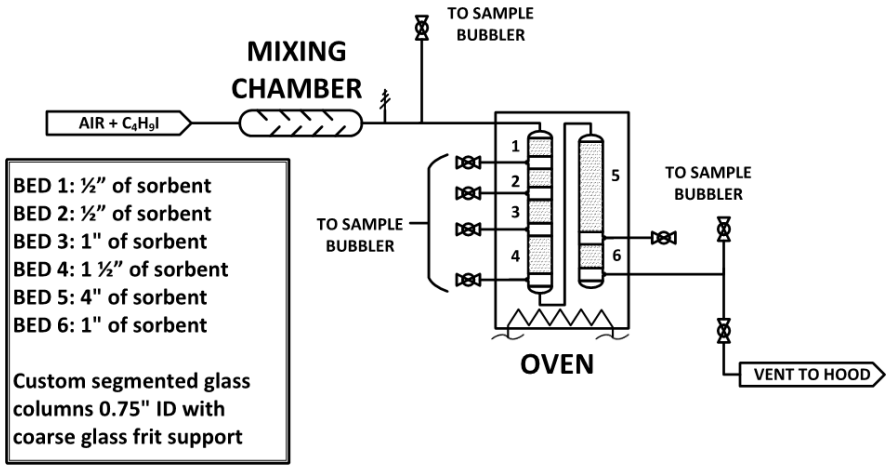

Figure 3-2. Detail of the INL sorbent bed, with starting bed depths for each segment.

Figure 3-3. Configuration of the INL sorbent bed inside the temperature-controlled oven.

When the gas stream is sampled, the entire gas stream is passed through impingers (for iodine scrubbing and analysis) or through sample tubes (for gas chromatography analysis). The removal efficiency and decontamination factor for a bed segment or combination of bed segments can be calculated using the inlet and outlet iodine species concentrations. The downstream sorbent beds are bypassed during gas sampling. The lost operating time for the downstream beds is tracked and recorded.

The iodine loadings on the sorbent and silver utilizations are determined by measurement of silver and adsorbed iodine using scanning electron microscope–energy dispersive spectroscopy or wet chemistry methods of sorbent digestion followed by sample analysis.

INL was provided reduced AgZ from ORNL, and the preparation of that material is described in Section 3.2. Silver-functionalized silica aerogel was provided by Pacific Northwest National Laboratory.

3.2 ORNL Deep Bed Testing

Silver mordenite was obtained from Molecular Products in an engineered pelletized form (Ionex-Type Ag 900 E16). It contains 9.5 wt% silver and has a 0.16 cm pellet diameter. Before use in testing, the sorbent material was reduced by exposure to a 4% H_2 blend in nitrogen at 270°C for 10 days. After reduction, the material was stored under argon to limit oxidation by air. Details of this procedure are provided by Anderson et al. (2012). The reduced AgZ had a measured bulk density of 0.84 g/cm^3.

A schematic of the deep bed test system is shown in Figure 3-4. The sorbent was contained within a glass column with an internal diameter of 2.73 cm. A total of 62.6262 g of Ag^0Z was poured into the glass column, with a measured column height of 11.5 cm. The first segment (1.9072 g) was separated from the remainder of the deep bed for ease of removal. The sorbent column was contained within an oven and held at 150°C. Figure 3-5 shows the sorbent column after testing.

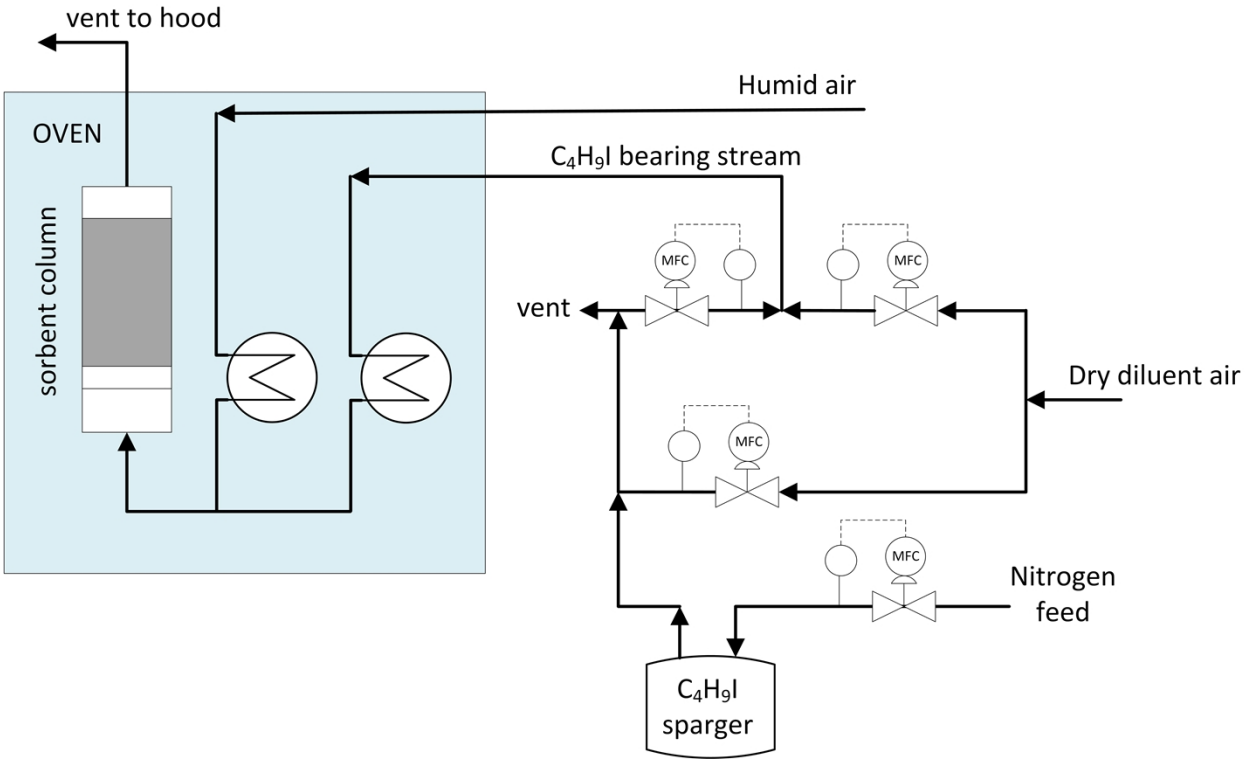

Figure 3-4. ORNL deep bed test system.

Figure 3-5. ORNL deep bed testing: AgZ column after exposure to 1 ppm iodobutane.

An iodobutane-bearing gas stream was generated by sparging liquid iodobutane with N_2 at a known flowrate. The N_2 stream leaving the gas sparger was assumed to be saturated with iodobutane at 22°C. The vapor pressure of iodobutane is such that this saturated stream required dilution before a small slipstream was pulled off and combined with the humid air stream. This humidified iodobutane-bearing gas stream was then passed through the sorbent column.

The vapor pressure of 1-iodobutane at 25°C is 1.83 kPa (13.8 mmHg) based on Antoine coefficients of [A = 5.94; B = 1,358.86; C = −58.95] (Stephenson and Malanowski 1987). Using the Antoine equation and the prescribed flowrates at the inlet to the column, the iodobutane concentration at 22°C was calculated as 1,097 ppb (1.097 ppm).

Before introduction into the sorbent bed, the humid air and iodobutane supply stream were piped through separate lines of tubing until they were blended. The system was visually examined for signs of corrosion before testing. All system lines were checked for leaks before testing.

The test proceeded continuously for a total of 99.16 hours online. Upon conclusion of the test, the AgZ bed was vacuumed out in discrete segments, and each segment was sent to the research reactor at University of Missouri for neutron activation analysis to determine iodine content.

3.3 ORNL Thin Bed Testing

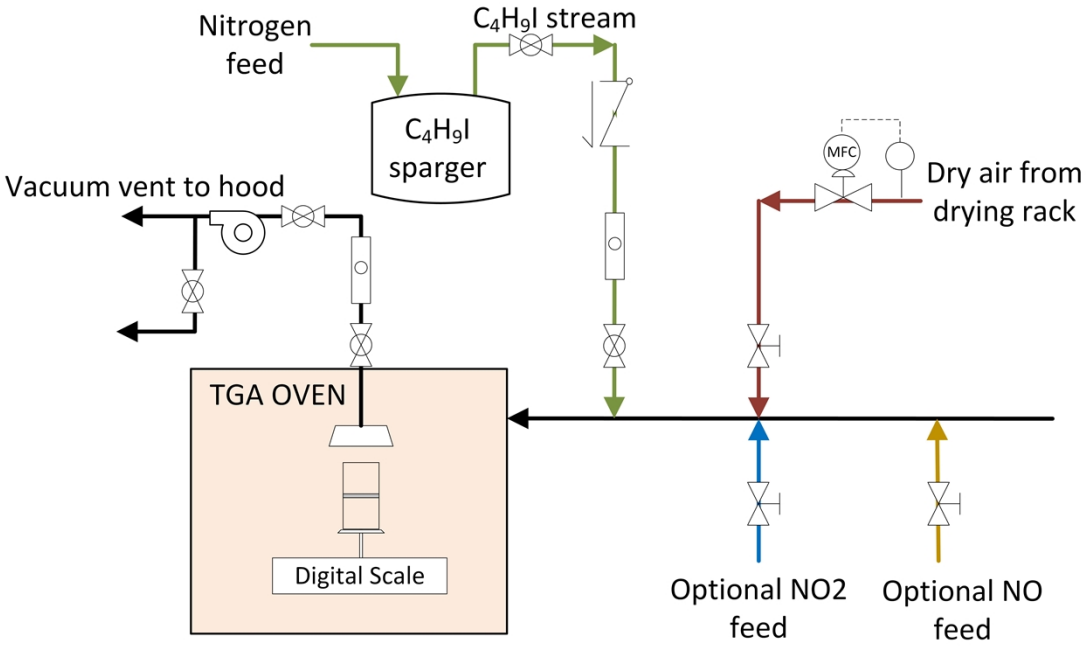

Figure 3-6. ORNL thermogravimetric analyzer (TGA).

Thin bed testing of iodobutane adsorption by AgZ was performed using a custom-built thermogravimetric analyzer. A thin bed of sorbent material (<2 g total weight) was contained within a temperature-controlled oven at 135°C. This thermogravimetric analyzer is designed to weigh the sorbent continuously as it is exposed to a dry gas stream bearing analytes of interest, in this case C_4H_9I. Operating in this manner allows for the iodine loading of the sorbent to be observed in real-time. Once the weight gain was observed to be less than 5 mg/g for a 24 hour period, the sorbent was assumed to be saturated. The sorbent was then purged with dry air for 24 hours to remove any physisorbed iodine. The C_4H_9I concentration of the gas stream was either 42 ppm or 10 ppm. The sorbent was held at 135°C, and the superficial gas velocity (as determined using the cross-sectional area of the sorbent bed) was 10 m/min.

4. RESULTS

The results presented here are compared to data obtained previously by INL and ORNL. In all cases, previous testing was conducted similarly to the testing described here. Detailed experimental details for previous tests can be found in the cited references. These data, comparisons, and conclusions should be considered preliminary at this early stage in the joint test plan. In some cases, results, comparisons, and conclusions are based on single, uncorroborated tests. Continued testing as prescribed in the joint test plan may confirm or supplement these results, comparisons, and conclusions.

4.1 ORNL Thin Bed Testing

Adsorption of iodine from iodobutane (42 ppm) by AgZ is shown in Figure 4-1 and is compared to adsorption curves obtained under the same test conditions for I_2 (25 ppm) and CH_3I (50 ppm). The observed weight gain for the iodobutane adsorption test was markedly higher (10.4 wt%) than for I_2 and CH_3I (6.7 and 7.4 wt%, respectively) even though the iodobutane concentration was lower than the CH_3I concentration. The iodobutane-loaded AgZ was sent for neutron activation analysis at the University of Missouri, which confirmed that the iodine concentration in the AgZ from the iodobutane test was 10.4 wt%. Therefore, the entirety of the observed weight gain was attributable to iodine adsorption and not to the adsorption of the organic moiety of the iodobutane, which has a greater mass than the organic moiety of the CH_3I and the I_2 (which has zero organic mass). This finding supports preliminary conclusions from organic iodide testing at INL that the chemisorption process apparently breaks up the organic iodide molecule, freeing the iodine to be chemisorbed on the sorbent, without resulting in significant adsorption of the organic moiety on the sorbent.

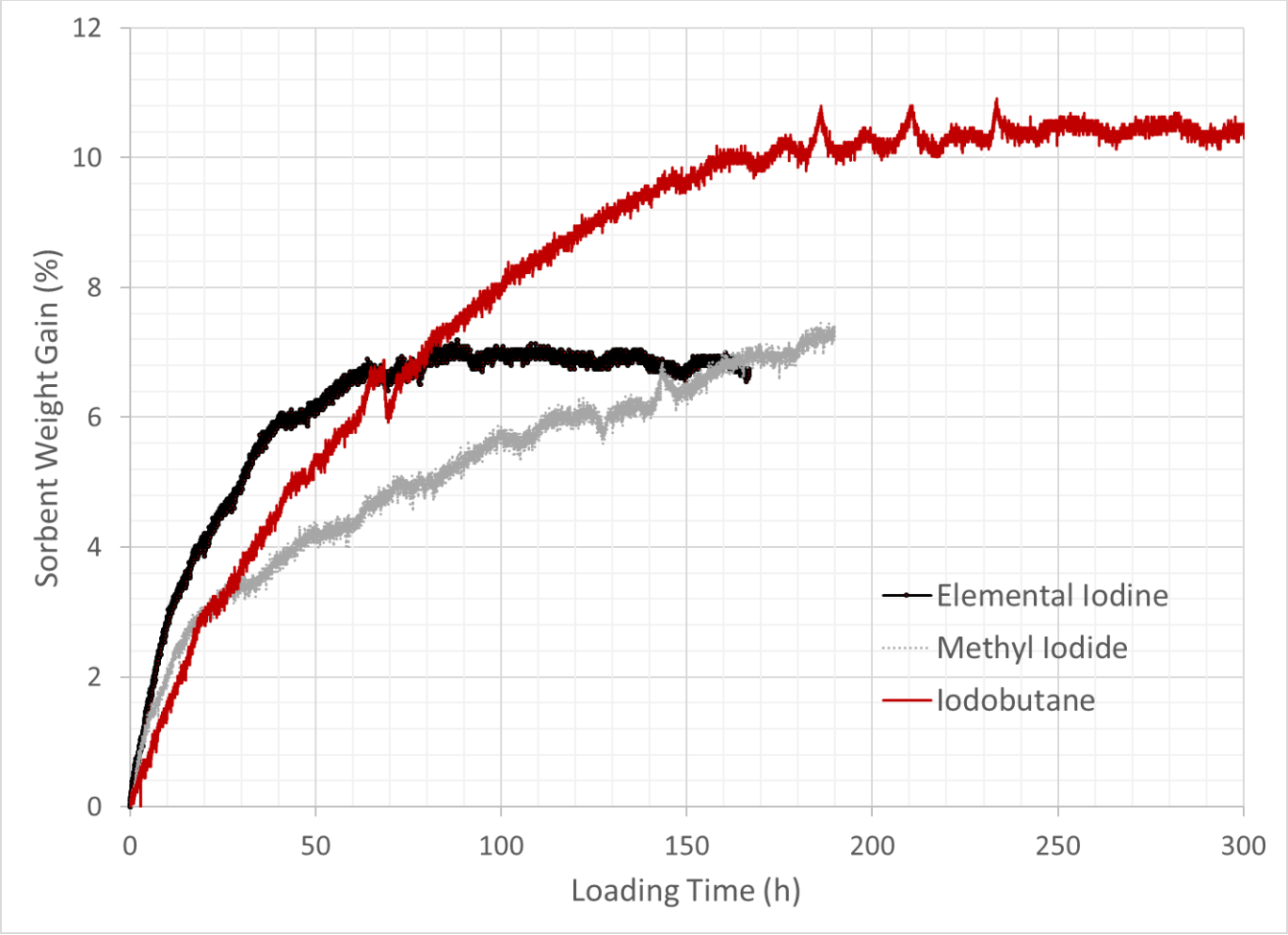

Figure 4-1. Thin bed loading curves for AgZ for varying iodine species.

Note, the sorbent reached maximum capacity for elemental iodine twice as quickly as it reached saturation for the organic iodides. After 80 hours of loading, additional I_2 adsorption by AgZ was minimal, although this point was not reached until 200 hours for CH_3I and 180 hours for iodobutane. This suggests that the adsorption rate for I_2 is fastest (even though the I_2 concentration as the driving force was lowest) and that

the next fastest was iodine adsorption from the one-carbon CH_3I, which also had the highest iodide concentration. The slowest iodine adsorption rate was from the four-carbon iodobutane, which had a lower iodide concentration than that of the CH_3I test. This informs questions 1 and 2. The adsorption rate appears to be slower for organic iodides than for I_2 and slowest for the longer-chain iodide. For the two organic iodides, the lower iodide concentration appears to have a slower adsorption rate.

Thin bed testing for iodobutane was conducted at both 42 and 10 ppm. The loading curves for each condition are shown in Figure 4-2. These preliminary results indicate that decreased concentration of iodobutane may slow its adsorption by AgZ and that the capacity of AgZ may be affected by iodine concentration in the feed gas. This data independently informs question 2.

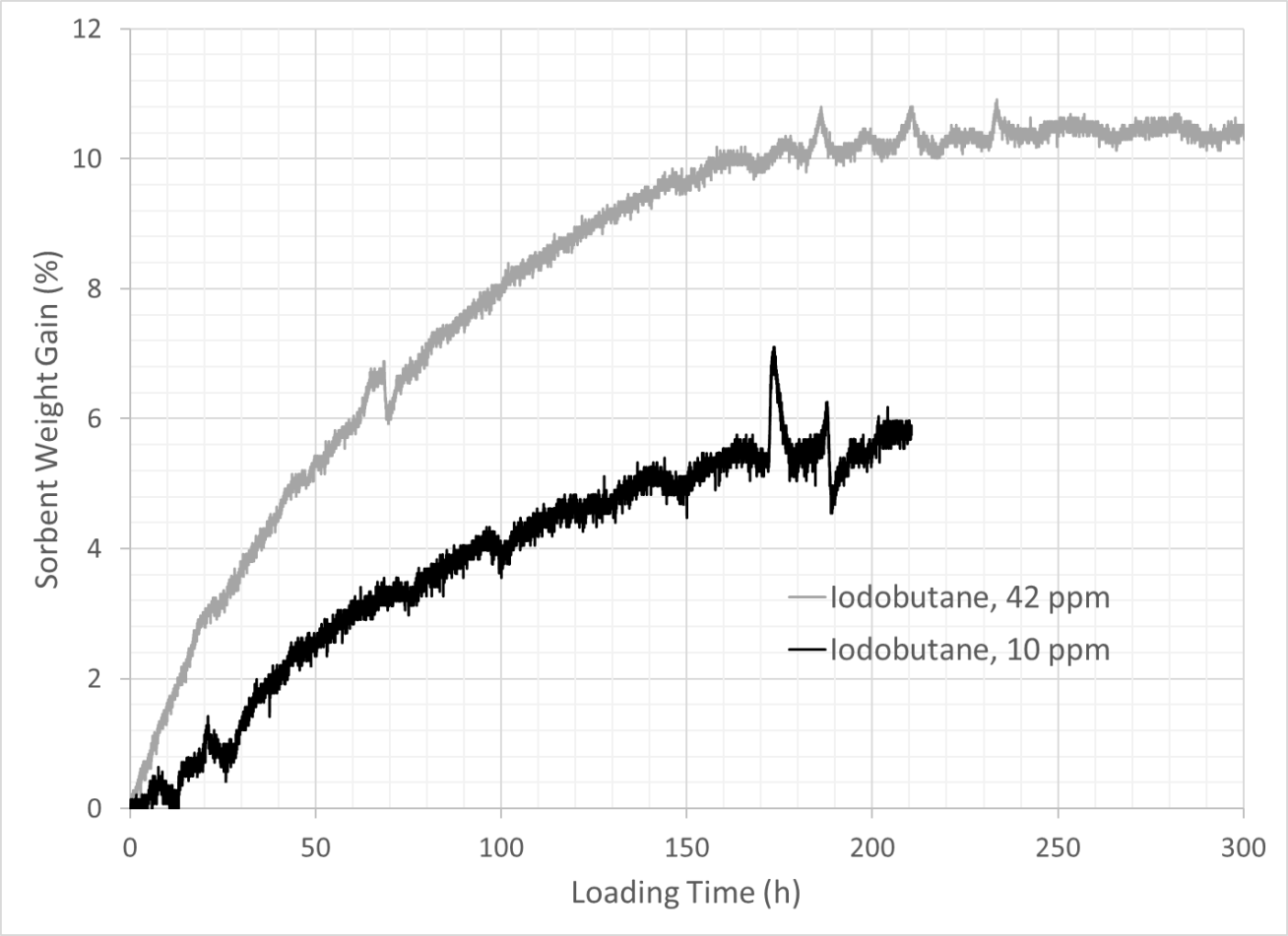

Figure 4-2. Iodobutane adsorption by AgZ at 42 and 10 ppm.

4.2 ORNL Deep Bed Testing

The iodine loading profile for I_2, CH_3I, and C_4H_9I is shown in Figure 4-3. The test duration does not allow for sorbent saturation, and the data should be interpreted accordingly. I_2 and CH_3I data were obtained from Jubin et al. (2017). The iodine content of the bed was determined by neutron activation analysis and represents the average iodine concentration of a segment of given length. In the figure, length of each individual segment is marked by horizontal lines, and the overall curve is plotted through the midpoint of the segment.

The iodine mass balances for these tests indicate that the total amount of iodine recovered on the sorbent deep beds does not always equal the total amount of iodine delivered to the bed. This discrepancy in mass balance has been investigated, but the cause is still not fully understood (Bruffey et al. 2018). For this reason, the data must be interpreted carefully. Table 4-1 shows the maximum observed iodine loading for each test (found in the first segment of the bed), the penetration depth of the sorbate, and the iodine mass balance. To normalize data to the varying mass balance, the percentage of recovered iodine found on the first 2 cm of the bed is provided.

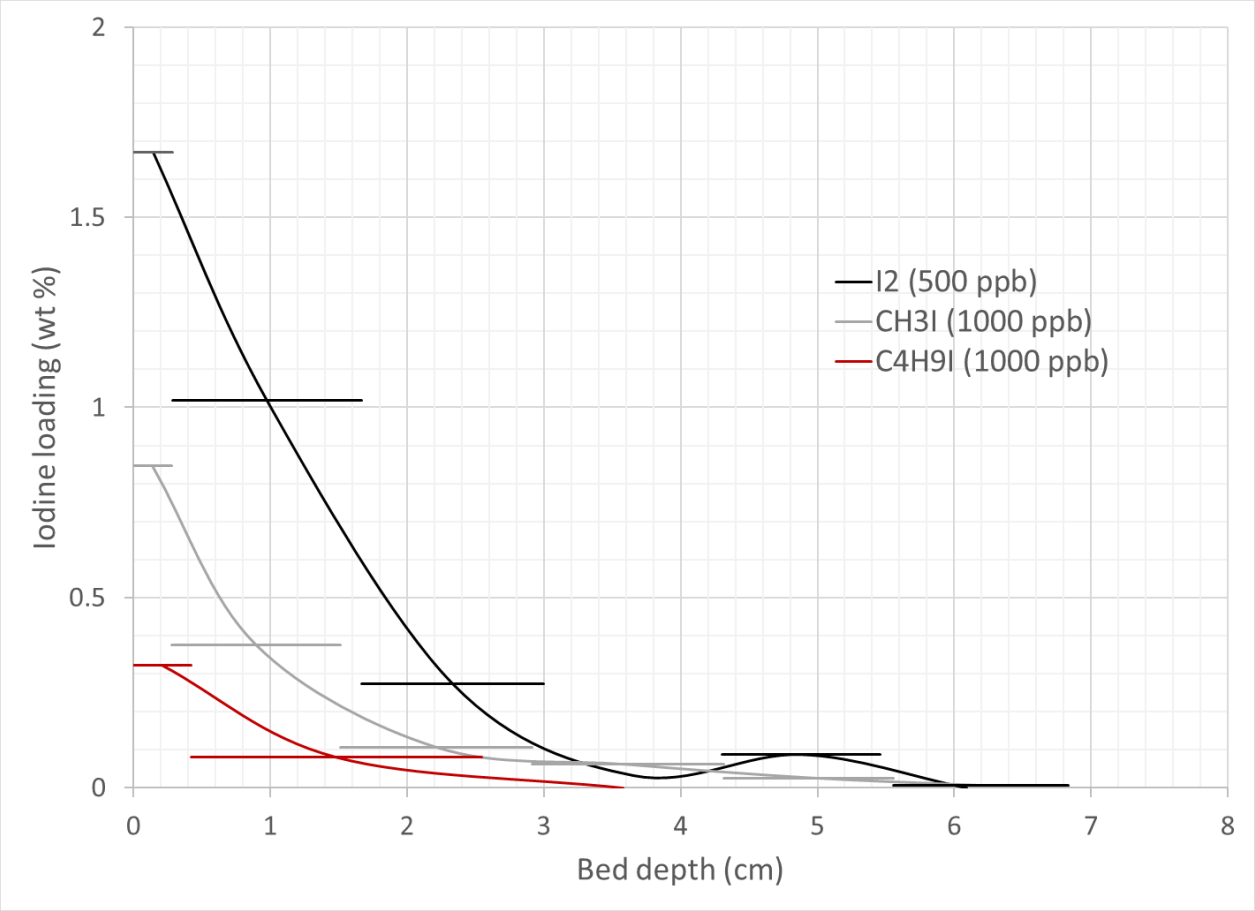

Figure 4-3. Iodine loading of AgZ as a function of bed depth and iodine speciation.

The loading of the first segment (which is unsaturated with iodine) was highest for elemental iodine and lowest for iodobutane. This does not correlate with the saturation capacities observed during the higher concentration thin bed testing (Figure 4-1) in which the highest loading was observed with iodobutane. However, when focusing only on the early loading of the thin beds (<20 hours) before sorbent saturation (and more in-line with the unsaturated deep bed testing discussed here), the early adsorption rates were highest for elemental iodine, followed by CH_3I, and the lowest was C_4H_9I. This is illustrated in Figure 4-4.

Table 4-1. ORNL deep bed data.

Test description	Maximum iodine loading (wt%)	Mass balance closure (%)	Penetration depth (cm)	Iodine adsorbed on first 2 cm (%)
I_2 (500 ppb)	1.7	100	5.5	85.8
CH_3I (1,000 ppb)	0.8	50	6.8	77.9
C_4H_9I (1,000 ppb)	0.3	31	2.5	100

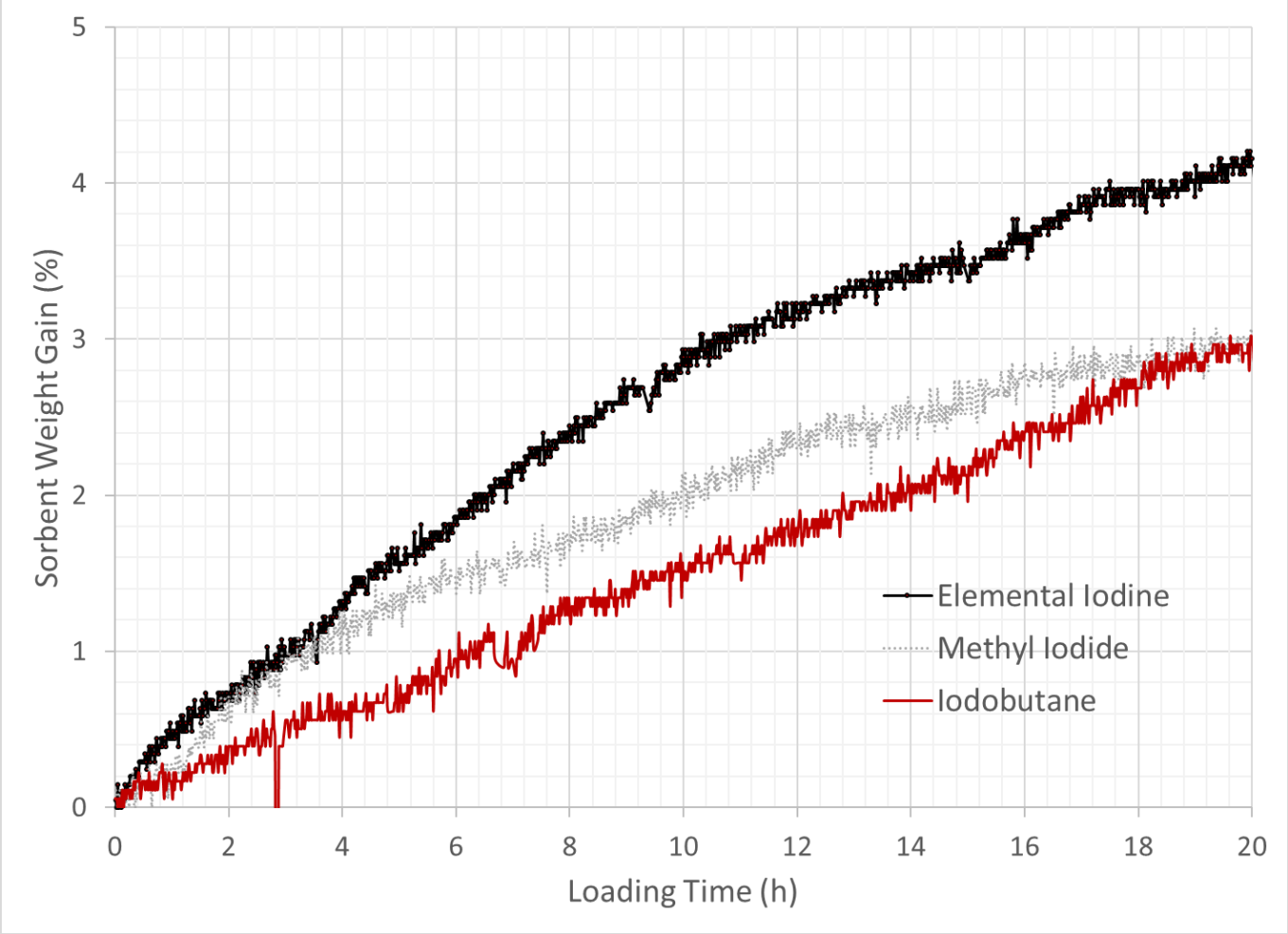

Figure 4-4. Thin bed loading of AgZ at times < 20 hours.

4.3 INL Deep Bed Data

In collaboration with the Off-gas Sigma Team, INL has performed iodine adsorption testing since 2009. The following sections illustrate the types of results from these tests and summarizes these test results for iodine and organic iodide capture using AgZ and AgAero.

4.3.1 Illustrations of Iodine DFs and MTZ Depth Measurements

One of the features of the INL deep bed test system is the ability measure the concentrations of iodides in the bed segment outlet gas streams, iodine DFs, and MTZs during sorbent tests. Figure 4-5 illustrates

gaseous iodobutane measurements from a recent long-term iodobutane test using AgAero with an average inlet concentration of 0.95 ppm in dry air with a nominal moisture dewpoint of −60°C. As expected, the shallow segments at the front of the sorbent bed (especially bed segments 1 and 2, with a total bed depth of about 2.54 cm [1 in.]) approach saturation quickly, even within 10 hours, and allow iodobutane to begin to break through those segments. Bed segments deeper in the sorbent bed break through more slowly (after 200 hours and about 2,000 hours for beds 3 and 4, respectively, with a total depth of about 9 cm [3.5 in.]). No iodobutane was detected during this 4,372 hour test at the outlets of the deepest bed segments 5 and 6, with a total depth of about 19 cm (7.3 in.). This was a typical trend for both I_2 and organic iodide tests, with both AgZ and AgAero sorbents.

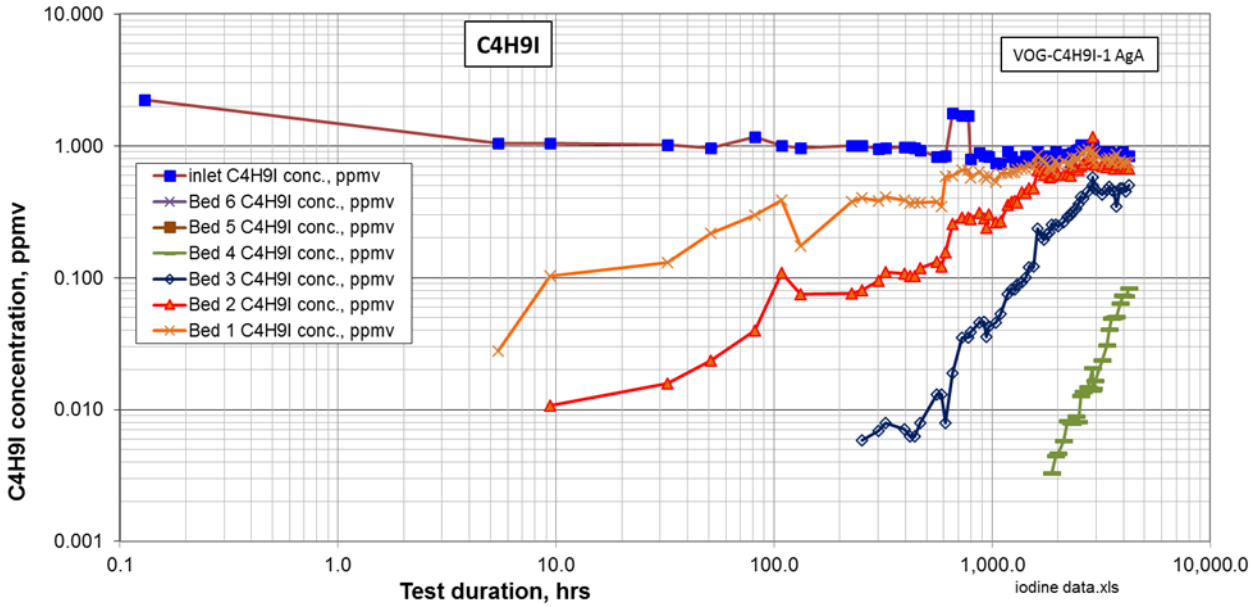

Figure 4-5. Iodobutane concentration trends in the bed outlet gas over time for Test VOG-C4H9I-1 Ag Aerogel (Soelberg 2019).

Figure 4-6 is also from the same recent iodobutane test with AgAero and shows an interesting result from the various organic iodide tests performed at INL. Inorganic iodide (such as I_2) was not added to the inlet gas, but it began to form and grow in the bed segment outlet gas. This result supports a conclusion about iodine capture from organic iodides: that the organic iodide molecule is broken up in the sorbent bed so that the iodine is freed to chemisorb via reaction with the Ag. When the sorbent approaches iodine saturation, many or most of the organic iodide molecules are still broken up; however, the released iodine passes out of the bed in the form of inorganic iodides, which are measured and reported as I_2. This trend, which was first reported in Haefner (2010) and further studied in Nenoff (2014), is observed with essentially all INL organic iodide tests; in some tests, practically 100% of the iodine that breaks through the sorbent after saturation is inorganic iodide such as I_2 instead of the original organic iodide.

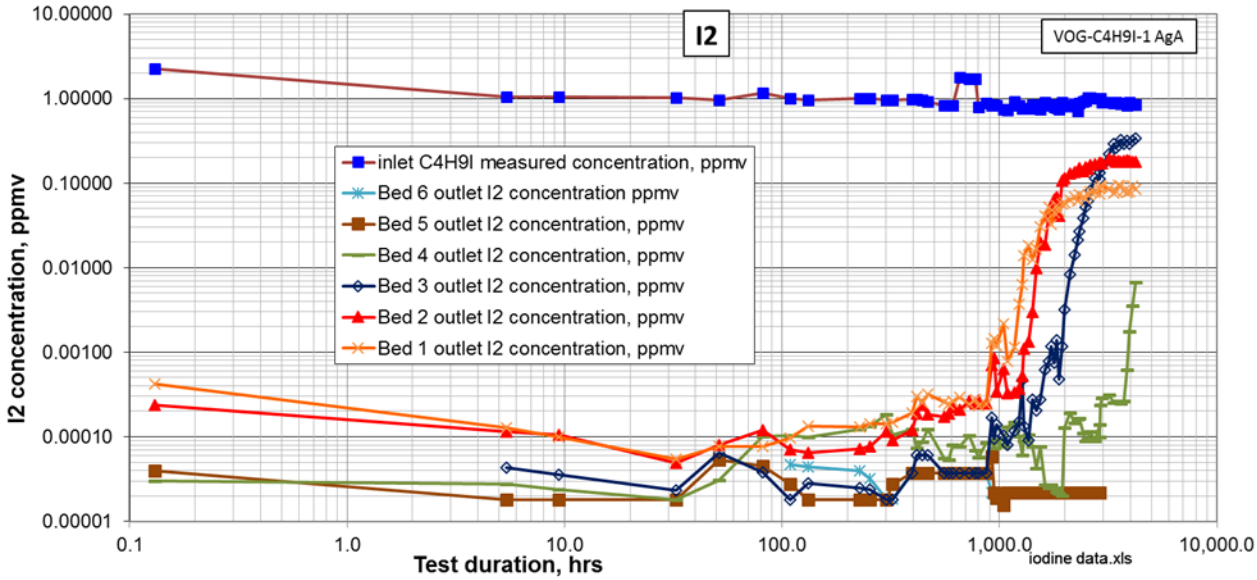

Figure 4-6. Bed segment outlet I_2 concentration trends over time for Test VOG-C4H9I-1 Ag Aerogel (Soelberg 2019).

Figure 4-7 illustrates the typical trends in iodine DFs for organic iodide tests. When the DF is calculated by including both the organic and inorganic iodides measured in the bed segment outlet gas, iodine DFs before the bed segment breakthrough generally trend high enough to meet or exceed minimum values expected to be needed to meet regulatory limits. These results provide proof-of-concept confirmation that engineered sorbent bed designs have potential to meet ^{129}I air emission regulatory limits.

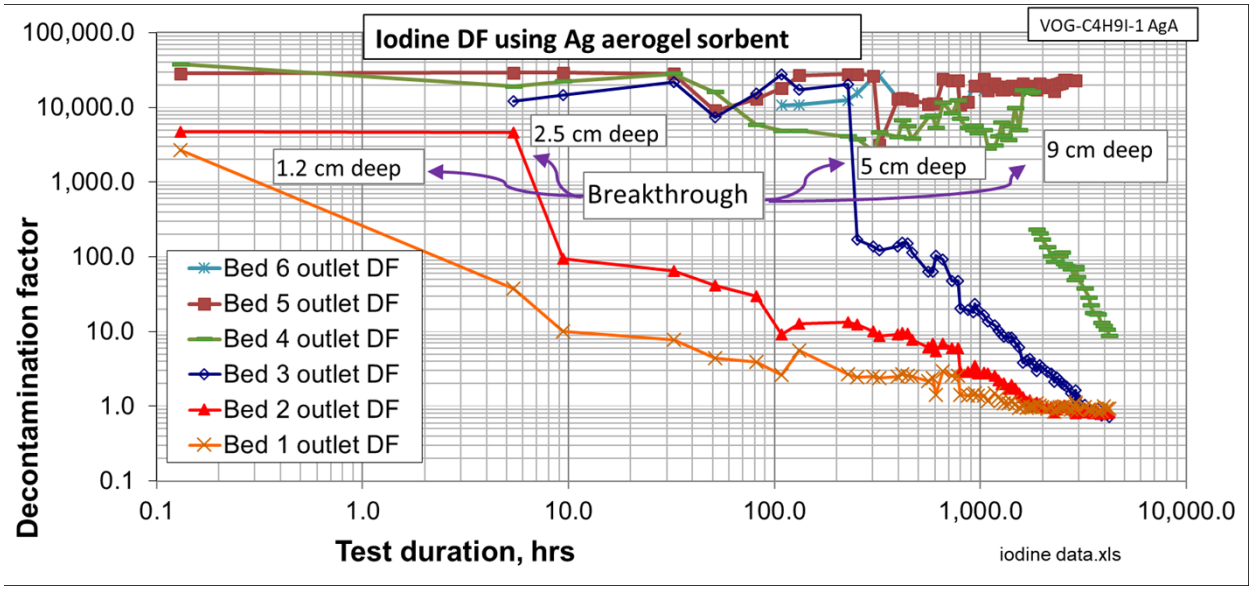

Figure 4-7. Total iodine DF trends over time for Test VOG-C4H9I-1 Ag Aerogel.

This figure also indicates how the MTZ depth is estimated. Using data from early in the long-term tests to estimate the MTZ is not recommended because the MTZ may take quite a while to become established, especially for low inlet iodide concentrations. The tendency for the sorbent to age over time of exposure to off-gas streams as has been reported by ORNL (Bruffey et al. 2013), Syracuse University, and Georgia

Tech (Choi 2019), and sorbent aging can further extend the depth of the MTZ (Soelberg 2012). In this test, the deepest MTZ depth is estimated to be about 9 cm (3.5 in.) as indicated at about hour 2,000, when the 9 cm (3.5 in.) deep bed 4 breaks through and the shallow beds 1 and 2 appear to have reached saturation.

4.3.2 Summary of Iodine and Organic Iodide Test Results

A summary of applicable INL deep bed testing performed over the past several years is shown in Appendix A. Selected test results are described in the following subsections.

AgZ and AgAero results are presented separately as the two sorbents differ in silver content, aging characteristics, particle size, and susceptibility to degradation from NO_x exposure. The differences in their silver content by weight (nominally 9.5 wt% in AgZ and 22 wt% in AgAero) also correlate to an observed difference in iodine capacity, with maximum capacities for AgZ and AgAero as high as 10 wt% and 20+ wt%, respectively. However, previous comparison of the two sorbents shows little difference in total iodine capacity once data is normalized to account for silver content in the sorbent beds (Jubin et al. 2017).

4.3.2.1 AgZ Test Results

Figure 4-8 shows AgZ sorbent capacities measured in iodine, methyl iodide, and iodobutane adsorption tests. In addition to grouping by iodide gas species, the different tests are grouped according to (a) whether the test was designed to emulate a DOG or VOG stream; (b) if the gas stream included NO_x gas species, water vapor, or both to bring the water dewpoint to typically between 0 and 20°C; and (c) if the tests were "short-term" or "long-term" tests. Short-term tests were typically a few hundred hours long and may not have been long enough to fully demonstrate the sorbent capacity or full depth of the MTZ that could occur in a full-scale long-term operation. In some cases, the sorbent capacities measured in these short-term tests trend lower than the corresponding capacities measured in ORNL thin bed tests. The long-term tests are limited to lower inlet iodide concentrations (representing potential VOG conditions) and have exceeded 2,000 hours (up to 10× longer than most of the short-term tests).

The line in this figure is not numerically determined from the graphed data but is placed merely to indicate that if the single VOG test in the upper left of the figure is differentiated from the other DOG tests, there appears to be a trend, even considering varying test conditions, that the AgZ capacity could slightly increase with increasing inlet iodide concentration. The capacity for the single VOG test, at about 12 wt% iodine, might be higher than the capacity for the other tests (and appropriately not included with the DOG data grouping) because of its ~10× longer test duration and because of its idealized bounding-level sorbent decay condition, since this test excluded NO_x, but added water (which, according to ORNL thin bed tests, can improve chemisorption of organic iodides). Excluding the higher VOG test sorbent capacity, the range of the capacities in AgZ for the DOG tests is between about 3 and 10 wt% iodine, regardless of inlet iodide concentration.

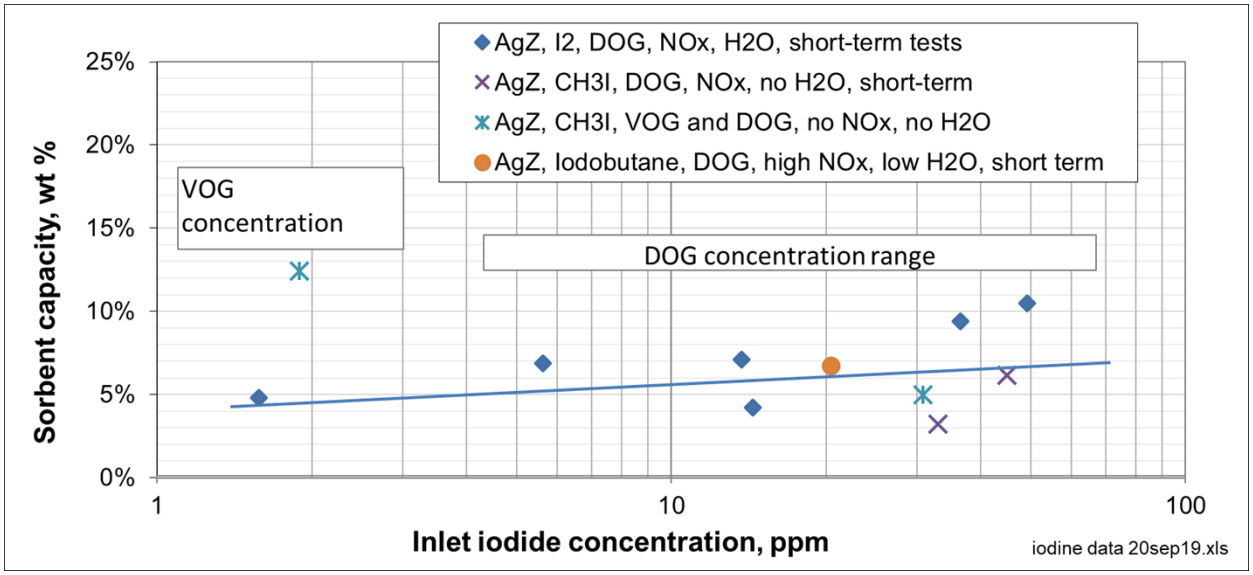

Figure 4-8. AgZ sorbent capacities for iodine measured in the INL deep bed tests.

Figure 4-9 shows the same data for iodine adsorption tests using AgZ in terms of the Ag utilization in the sorbent. This figure shows the same trends that were shown for the AgZ sorbent capacity. These data suggest that the one VOG test, with measured Ag utilization at 100%, should not be grouped with the DOG tests; and that the Ag utilization tends to increase with increasing inlet iodine concentration. The Ag utilizations for the short-term DOG tests appear to rise with increasing iodide concentration and range from about 20 to 60%. These less-than-100% Ag utilization measurements could reflect sorbent aging during the tests or relatively shorter test durations that may not have been long enough for the sorbent to reach full capacity.

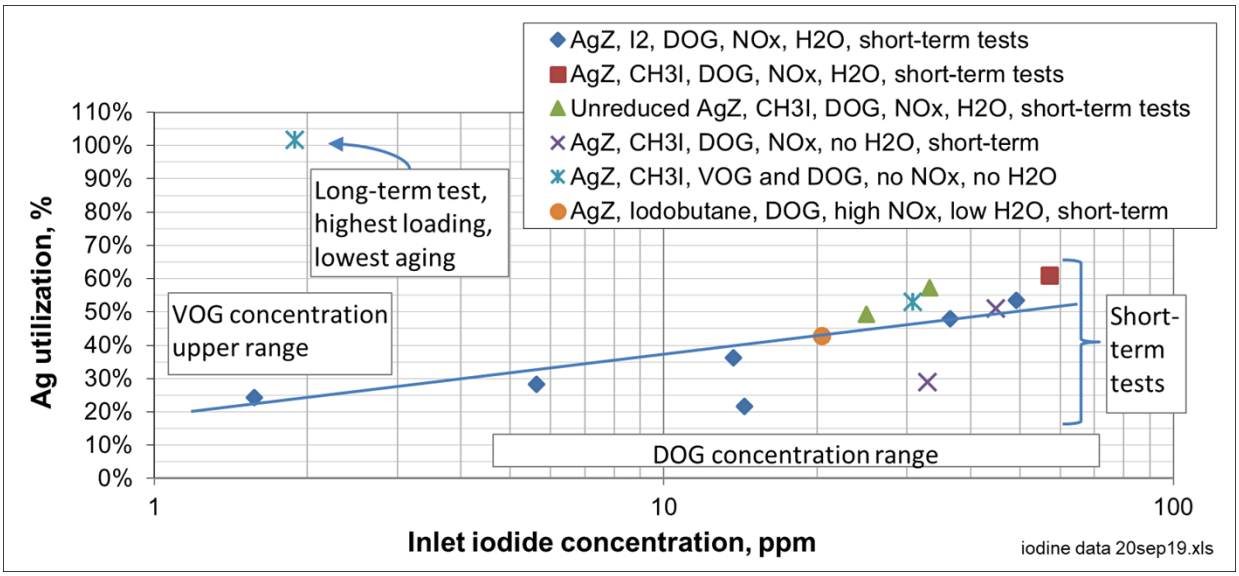

Figure 4-9. Silver utilization in the AgZ sorbent.

These two figures of AgZ capacity and AgZ utilization inform question 4. Based on these deep bed tests, there does not seem to be a recognizable, significant impact of different organic iodides, compared to I_2, on

AgZ capacity for iodine. The scatter in the range of 3–10 wt% iodine capacity (20–60% Ag utilization) may be due to other factors that can contribute to aging of the sorbent during the test. Future testing according to the joint test plan may enable these conclusions to be updated.

Figure 4-10 shows the depths of the MTZ for the different AgZ adsorption tests. Most MTZ depths were about 10 cm (4 in.), regardless of inlet iodide concentration. However, a few higher-iodide concentration tests indicate MTZ depths as high as 20 cm (8 in.), especially for two tests that included NO_x. These results inform questions 1, 2, and 7 because the length of the MTZ reflects the adsorption rate.

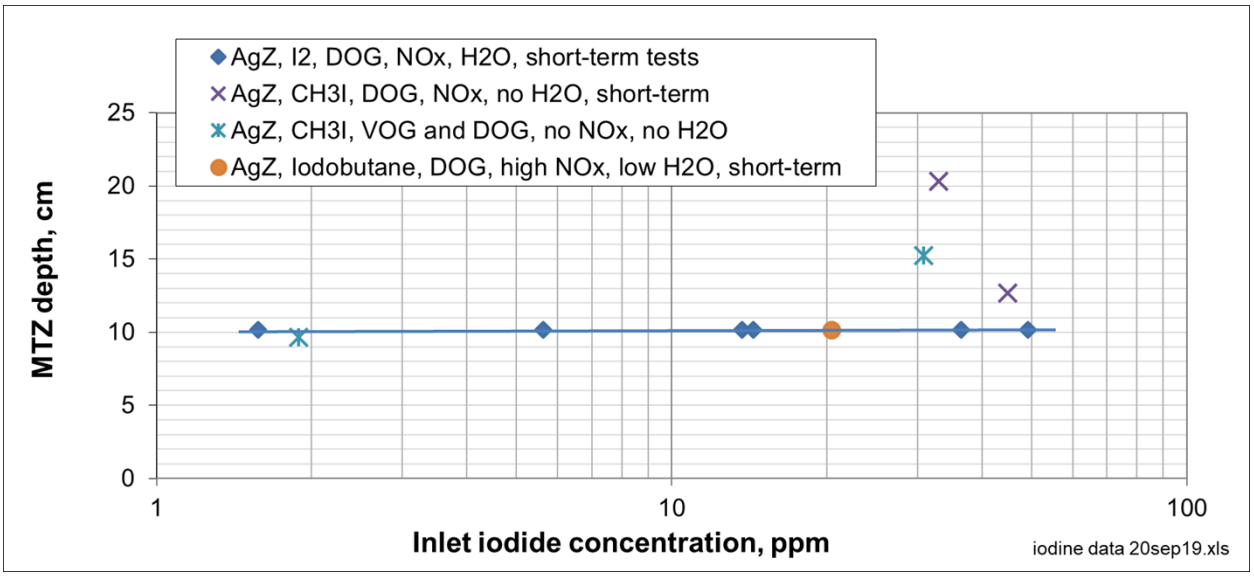

Figure 4-10. MTZ depths for the AgZ sorbent tests.

4.3.2.2 Ag-Aerogel Test Results

Figure 4-11 shows the corresponding sorbent capacity data for AgAero sorbent. The trends are generally similar to those observed with AgZ. The highest sorbent capacity, 22 wt% iodine, was measured for a long-term test using iodobutane and excluded NO_x and water; consequently, this test may not have experienced the same degree of aging that can occur when the sorbent is exposed to NO_x and water vapor. A second grouping of tests simulating DOG conditions with highest NO_x were observed to have lower iodine capacities (between 5 and 15 wt% iodine). A third grouping of three tests suggests that without otherwise being affected by test durations or higher or lower sorbent aging conditions, the AgAero capacity could trend higher for higher inlet iodide concentrations and may reach capacities between 11 and 20 wt% iodine.

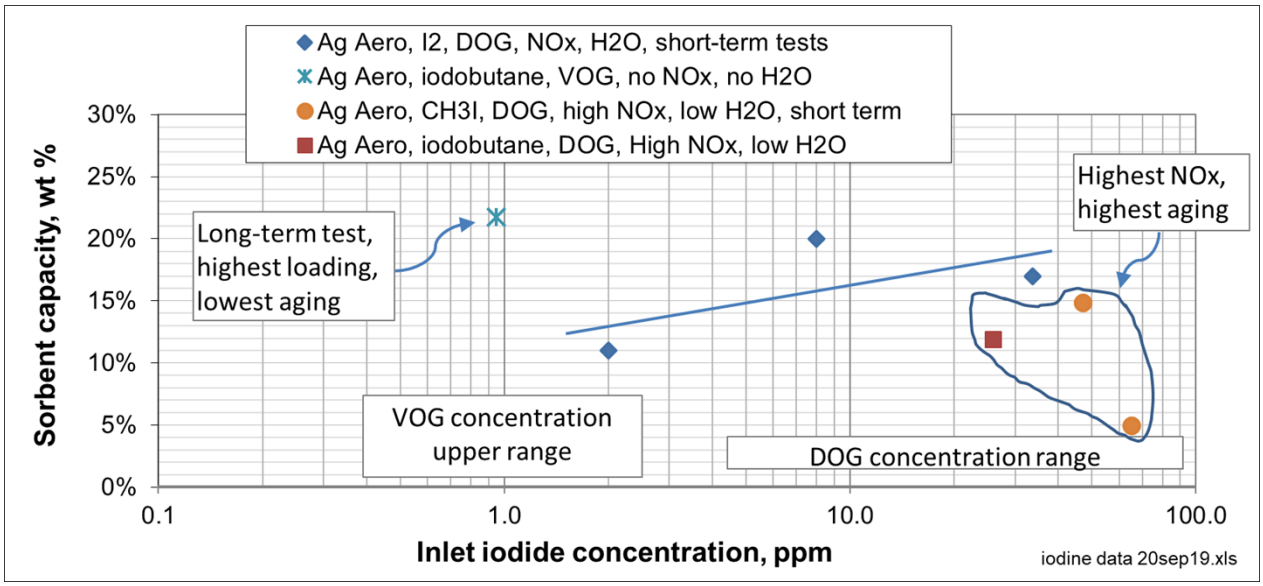

Figure 4-11. Ag Aerogel sorbent capacities for iodine.

Figure 4-12 shows the corresponding Ag utilization results for the Ag Aerogel tests. The Ag utilization trends for these tests are the same as the iodine capacity trends. The highest Ag utilization, at about 70%, was for the long-term VOG test. The lowest Ag utilization range, at between 10 and 40%, was for the short-duration DOG tests with higher potential sorbent aging. The other DOG tests suggest that Ag utilization can trend higher with increasing inlet iodide concentrations, with a range between about 30 and 57%.

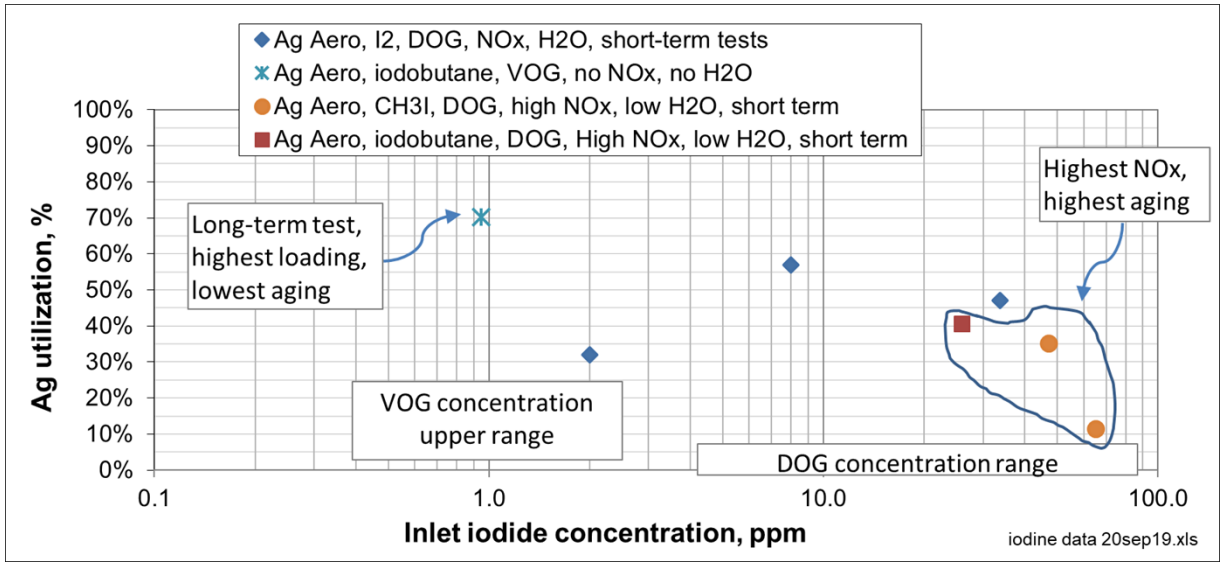

Figure 4-12. Ag utilization in the Ag Aerogel sorbent.

These two figures of AgAero capacity and AgAero utilization inform question 4, with similar conclusions drawn as for the AgZ sorbent. There does not seem to be a recognizable, significant impact of different organic iodides on AgAero capacity for iodine. The single VOG test with the high iodine capacity of about 22 wt% (100 Ag utilization) may have benefited from low sorbent aging. The grouping with lower iodine capacities and lower Ag utilizations may have resulted from higher silver-oxide producing conditions

(with higher NO_x levels). The middle grouping of I_2 tests suggests that increasing iodide concentration can increase the AgAero capacity, although there is considerable scatter. Future testing according to the joint test plan may enable these conclusions to be updated.

The AgZ and AgAero Ag utilizations, when the outlying tests are excluded, both show middle-range Ag utilizations between 20 and 60%. These results support the premise that the iodine adsorption performance of the two sorbents is close to equivalent when the capacity is normalized for silver content in the sorbents (Jubin et al. 2017).

Figure 4-13 shows the estimated MTZ depths for the AgAero tests. Like for AgZ, the MTZ depth was measured at 10 cm (4 in.) for most of the tests. The long-term VOG test, with lower iodide concentration and lower sorbent aging, had an estimated MTZ depth of about 7.6 cm (3 in.). Two higher iodide concentration tests, with higher potential sorbent aging potential, had estimated MTZ depths of 20 cm (8 in.). This figure suggests a trend of increasing MTZ depth with increasing inlet iodide concentration. However, multiple experimental parameters were varied across the tests being compared, which prevents clear resolution of the effect of inlet concentration on the MTZ. These results inform questions 1, 2, and 7 because the length of the MTZ reflects the adsorption rate.

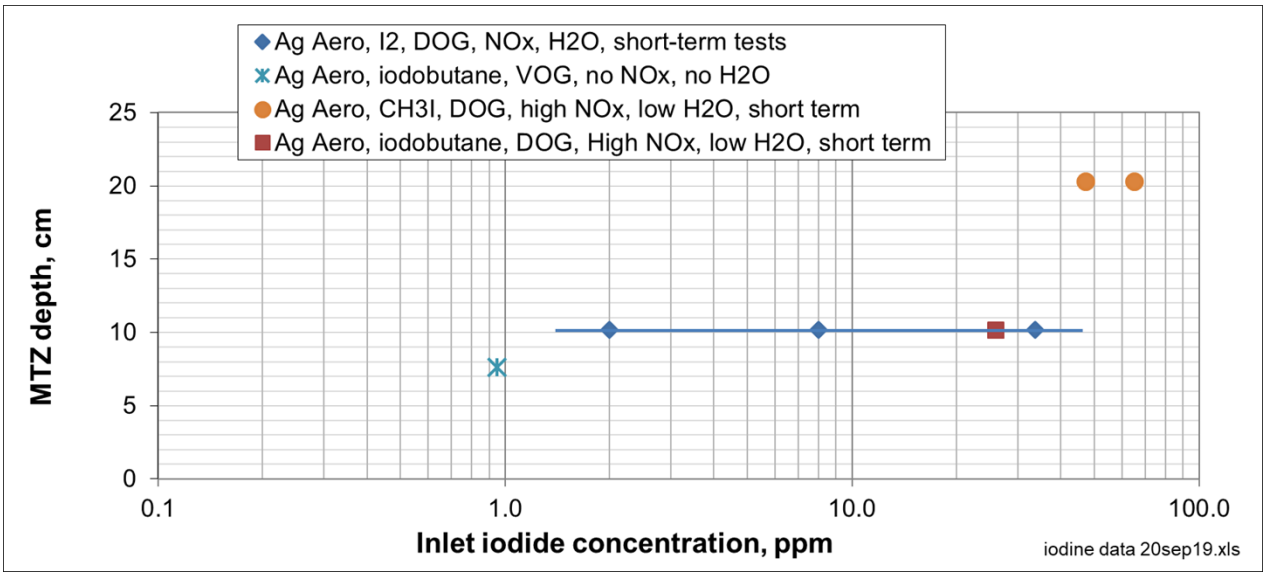

Figure 4-13. Mass transfer zone depths for the Ag Aerogel sorbent tests.

4.3.2.3 Iodine Decontamination Factor Measurements

Figure 4-14 shows the iodine DF measurements for both the AgZ and Ag Aerogel sorbent tests. The DFs were generally satisfactory for all tests at all conditions, with just a few tests with DFs under 1,000. In many cases, the DF values result from using detection limit data for the organic iodide and diatomic iodine measurements, so true DFs may even be higher. How representative these DF values are for use in designing full scale sorbent beds depends on interferences, such as wall effects, in these small-scale tests and on potential gas channeling if larger-scale beds are not designed to minimize such effects. DFs for larger-scale beds should be confirmed.

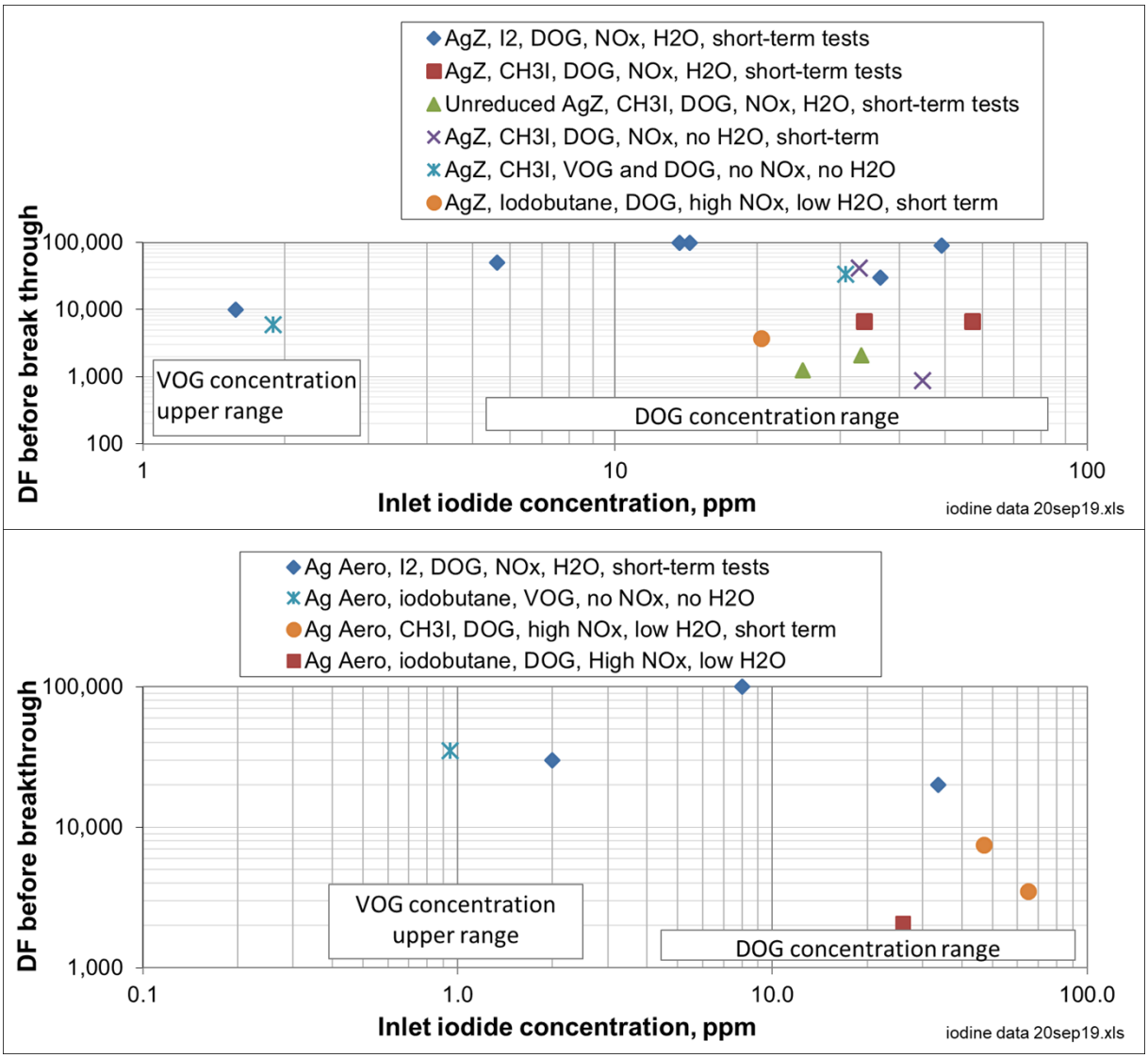

Figure 4-14. INL deep bed test DF measurements.

5. SUMMARY AND CONCLUSIONS

ORNL and INL have begun executing a multiyear joint test plan intended to provide a better understanding of organic iodide adsorption from VOG conditions. In this fiscal year, ORNL conducted thin bed testing on the adsorption of CH_3I and C_4H_9I by AgZ and deep bed testing on the adsorption of C_4H_9I by AgZ. INL has conducted extended duration deep bed testing on the adsorption of C_4H_9I and CH_3I by AgZ and AgAero. Because this is the first year of this effort, many of the conclusions should be considered preliminary. The data provided in this report will be used to answer four of the seven primary objectives of the test plan.

First, this testing provides data on the adsorption rate as a function of hydrocarbon chain length. Both thin and deep bed testing by ORNL show that organic iodides may be adsorbed up to 50% more slowly than elemental iodine. However, the adsorption rates for the organic iodides tested thus far (CH_3I and C_4H_9I)

cannot be resolved. Additional testing with iodododecane ($C_{12}H_{25}I$) will be required to better determine the effect of hydrocarbon chain length on organic iodide adsorption.

In contrast, the adsorption rate does not seem to be strongly affected by hydrocarbon chain length when the adsorption rate is related to the MTZ in the INL deep bed tests. MTZ depth begins to be more scattered at higher inlet iodide concentrations but otherwise seems to average about 10 cm regardless of sorbent and regardless of iodide species. This should be addressed in future studies.

Second, this testing provides initial data on the rate of organic iodide adsorption as a function of concentration. Preliminary thin bed testing on the adsorption of C_4H_9I at two concentrations (42 and 10 ppm) shows that the difference in initial adsorption rate between these two concentrations is marked. Further thin bed testing with CH_3I and $C_{12}H_{25}I$ at varied concentrations will be conducted in the near-term by ORNL to better understand the rate of organic iodide adsorption as a function of hydrocarbon chain length.

When the adsorption rate is related to mass transfer zone in deep bed tests, the concentration does not seem to significantly affect the MTZ (especially aging caused by high NO_x) once other factors are accounted for.

Third, limited data on the saturation concentration of long-chain iodides on silver-based sorbents has been obtained by both ORNL and INL, and some differences were observed between the two laboratories and across different organic iodine species. Results indicate that once the iodine loading is normalized to Ag content, both sorbents have about the same capacity. Aging also affects the sorbent capacity, as has been demonstrated in prior ORNL testing and Syracuse University testing (Choi 2019).

Finally, DFs over a fixed bed length have been obtained by INL for elemental iodide, CH_3I, and C_4H_9I. The data obtained show a high degree of scatter. When the DF is calculated by including both the organic and inorganic iodides measured in the bed segment outlet gas, iodine DFs before bed segment break through, the DFs still generally trend high enough to meet or exceed minimum values expected to meet regulatory limits. These results provide proof-of-concept confirmation that engineered sorbent bed designs have potential to meet ^{129}I air emission regulatory limits.

Both ORNL and INL continue to execute the multiyear joint test plan in close collaboration. Continued success is expected as additional data is obtained and key questions regarding organic iodide adsorption by silver-based sorbents are answered. It is expected that completion of the test plan will result in the ability to provide reliable engineering designs for the removal of iodine from VOG streams.

6. REFERENCES

Anderson, K. K., S. H. Bruffey, D. L. Lee, R. T. Jubin, and J. F Walker. 2012. Iodine Loading of Partially Reduced Silver Mordenite. Report No. FCRD-SWF-2013-000079. US Department of Energy Separations and Waste Forms Campaign, December 28.

Bruffey, S. H., R. T. Jubin, K. K. Anderson, and J. F. Walker. 2013. “Aging and Iodine Loading of Silver-Functionalized Aerogels.” In *Proceedings of GLOBAL 2013: International Nuclear Fuel Cycle Conference-Nuclear Energy at a Crossroads*.

Bruffey, S. H., B. B. Spencer, D. M. Strachan, R. T. Jubin, N. R. Soelberg, and B. J. Riley. 2015. A Literature Survey to Identify Potentially Problematic Volatile Iodine-Bearing Species Present in Off-Gas Streams, FCR&D-MRWFD-2015-000421, ORNL-SPR-2015/290, INL/EXT-15-35609, June 30.

Bruffey, S. H., R. T. Jubin, and J. A. Jordan. 2018. “Quantify the Extent of Physisorption on Silver Based Sorbents under VOG Conditions,” ORNL/SPR-2018/1066. Oak Ridge National Lab, Oak Ridge, TN

Choi, S., Y. Nan, A. Wiechert, A. P. Ladshaw, S. Yiacoumi, C. Tsouris, L. L. Tavlarides. 2019. Aging Study of Ag^{o}Z and Ag^{o}-Aerogel in the Presence of Off-Gas Streams. Global 2019, Seattle, WA.

Haefner, D., and N. Soelberg. 2009. Experimental Sorption Testing of Elemental Iodine on Silver Mordenite, AFCI-SEPA-PMO-MI-EV-2009-000193, INL/EXT-09-16837, September 28.

Haefner, D. R. and T. L. Watson. 2010. Summary of FY2010 Iodine Capture Studies at the INL, INL/EXT-10-19657, August.

Jubin, R. T, N. R. Soelberg, D. M. Strachan, and G. Ilas. 2012. Fuel Age Impacts on Gaseous Fission Product Capture During Separations, FCRD-SWF-2012-000089, September 21.

Jubin, R. T., D. M. Strachan, and N. R. Soelberg. 2013. Iodine Pathways and Off-Gas Stream Characteristics for Aqueous Reprocessing Plants—A Literature Survey and Assessment, FCRD-SWF-2013-000308, ORNL/LTR-2013/383, INL/EXT-13-30119, September 15.

Jubin, R. T., J. A. Jordan, and S. H. Bruffey. 2017. Performance of Silver-Exchanged Mordenite and Silver-functionalized Silica-Aerogel under Vessel Off-gas Conditions, ORNL/TM-2017/477. Oak Ridge National Laboratory, Oak Ridge, TN. September.

Jubin, R. T., S. H. Bruffey, N. R. Soelberg, and A. K. Welty. 2018. Joint Test Plan for the Evaluation of Iodine Retention for Long-Chain Organic Iodides, NTRD-MRWFD-2018-000212, ORNL/SPR-2018/781, February 28.

Nenoff, T., M. Rodriguez, N. Soelberg, and K. Chapman. 2014. Silver-Mordenite for Radiologic Gas Capture from Complex Streams: Dual Catalytic CH3I Decomposition and I Confinement, Microporous and Mesoporous Materials, MICMAT6530, INL/JOU-14-31276, May 9.

Soelberg, Nick and Tony Watson. 2012. Iodine Sorbent Performance in FY 2012 Deep Bed Tests, FCRD-SWF-2012-000278, INL/EXT-12-27075, August 31.

Soelberg, Nick and Tony Watson. 2014a. Phase 1 Methyl Iodide Deep-Bed Adsorption Tests, INL/EXT-14-32917, August 22.

Soelberg, N., and T. Watson. 2014b. “Phase 2 Methyl Iodide Deep-Bed Adsorption Tests, FCRD-SWF-2014-000273, INL/EXT-14-33269, September 30.

Soelberg, N., and T. Watson. 2015. FY-2015 Methyl Iodide Deep-Bed Adsorption Test Report, FCRD-MRWFD-2015-000267, INL/EXT-15-36817, Idaho National Laboratory, September 30.

Soelberg, N., and T. Watson. 2016. FY-2016 Methyl Iodide Higher NOx Adsorption Test Report, FCRD-MRWFD-2016-000352, INL/EXT-16-40087, Idaho National Laboratory, September 29.

Soelberg, N. 2017. Iodo-dodecane Spiking and Analysis for Iodine Adsorption Testing, NTRD-MRWFD-2017-000304, INL/EXT-17-41350, March 1.

Soelberg, N., A. K. Welty, and S. Thomas. 2018. Iodobutane Deep Bed Adsorption Test Report, NTRD-MRWFD-2018-000190, INL/EXT-18-45120, April.

Soelberg, N., A. K. Welty, and S. Thomas. 2019. Iodine Capture from Iodobutane in Vessel Off-gas, INL/EXT-19-53741, April.

Stephenson, R. M., and S. Malanowski. 1987. “Properties of organic compounds.” *Handbook of the Thermodynamics of Organic Compounds*. Springer, Dordrecht. 1–471.

APPENDIX A

Table A-1. Summary results of organic iodide adsorption tests.

Run Number	AgZ-1	AgZ-2	AgZ-3	AgZ-6	AgZ-5	AgZ-4	Ag-1	Ag-2	Ag-3
Simulate what off-gas?	DOG	DOG	DOG	DOG	DOG	DOG	DOG	DOG	DOG
Sorbent	AgZ	AgZ	AgZ	AgZ	AgZ	AgZ	Ag Aero	Ag Aero	Ag Aero
Target iodide	**I2**	**I2**	**I2**	**I2**	**I2**	**I2**	**I2**	**I2**	**I2**
Average measured iodide concentration, ppmv	1.6	5.6	14.4	13.7	36.5	49.2	2.0	33.7	8.0
H2O conc, %	1.5%	1.5%	1.5%	1.5%	1.5%	1.5%	1.5	1.5	1.5
H2O dewpoint, deg. C	11%	11%	11%	11%	11%	11%	18	18	18
NO conc., ppmv	801	800	801	801	801	801	801	801	801
NO2 conc., ppmv	801	800	801	801	801	801	801	801	801
Balance (air or N2)	Air	Air	Air	Air	Air	Air	N2	N2	N2
Sorption gas velocity, m/min	10	10	10	10	10	10	10	10	10
Maximum sorbent weight change, %	4.8	6.9	4.2	7.1	9.4	10.5	11%	17%	20%
Cumulative test duration, hrs	140	229	36	109	55	48	242	64	162
Iodine loadings from SEM/EDS									
Bed 1	4.8%	6.9%	4.2%	7.1%	9.4%	11%	11%	17%	20%
Silver utilization									
Bed 1	24%	28%	22%	36%	48%	53%	32%	47%	57%
Max DF before breakthrough	10,000	50,000	100,000	100,000	30,000	90,000	30,000	20,000	100,000
Average conversion of iodide to I2 in inlet gas, %	---	---	---	---	---	---	---	---	---
Max conversion of bed outlet iodide to I2, %	---	---	---	---	---	---	---	---	---
Mass transfer zone depth, inches	4	4	4	4	4	4	4	4	4
Reference	Soelberg 2012								

Table A-1. Summary results of organic iodide adsorption tests (continued).

Run Number	CH3I 5 33 ppm CH3I w/o NOx H2O	CH3I 6 33 ppm CH3I w/ NOx, w/o H2O	CH3I 7 AG 33 ppm CH3I w/ NOx, H2O	CH3I-12 AgZ 50 ppm CH3I w/ NOx, no H2O	CH3I-17 High NOx Ag Aerogel	CH3I-18 High NOx Ag Aerogel	C4H9I-1 Hi NOx AgA	C4H9I-2 Hi NOx AgZ	VOG-C4H9I-1 AgA	VOG-CH3I-2 AgZ
Simulate what off-gas?	DOG	DOG	DOG	DOG	DOG	DOG	DOG	DOG	**VOG**	**VOG**
Sorbent	AgZ	AgZ	Ag Aero	AgZ	Ag Aero	Ag Aero	Ag Aero	AgZ	Ag Aero	AgZ
Target iodide	CH3I	CH3I	CH3I	CH3I	CH3I	CH3I	C4H9I	C4H9I	C4H9I	CH3I
Average measured iodide concentration, ppmv	31	33	24	45	47	65	26	20	0.95	1.89
H2O conc, %	0.0003%	0.0300%	1.80%	0.0003%	0.6%	0.6%	0.6%	0.6%	0.0003%	0.58%
H2O dewpoint, deg. C	-60	-60	20	-60	0	0	0	0	-60	0
NO conc., ppmv	0	822	824	1,000	3,326	3,268	3,237	3,236	0	0
NO2 conc., ppmv	0	822	824	1,000	5,682	9,635	9,675	10,013	0	0
Balance (air or N2)	Air	Air	Air	Air	Air	Air	Air	Air	Air	Air
Sorption gas velocity, m/min	4.3	4.3	4.3	4.3	4.3	4.4	4.4	4.4	10	10
Maximum sorbent weight change, %	5.0%	3.2%	---	5.8%	1.8%	-3.5%	0.9%	0.2%	---	---
Cumulative test duration, hrs	424	462	260	523%	179	314	429	282	4,372	2,092
Iodine loadings from SEM/EDS	% adsorbed iodine of mass of initial sorbent									
Bed 1	5.0%	---	---	6.2%	15%	5.0%	12%	6.8%	21%	12%
Silver utilization	%									
Bed 1	53%	29%	---	51%	35%	12%	41%	43%	66%	102%
Max DF before breakthrough	33,858	41,767	134	871	7,494	3,509	2,067	3,767	35,000	6,000
Average conversion of iodide to I2 in inlet gas, %	---	3.3%	1.8%	0.9%	1.2%	1.4%	0.28%	0.19%	0.33%	0.43%
Max conversion of bed outlet iodide to I2	5.0%	99.9%	0.7%	99.4%	100.0%	100.0%	99.9%	99.97%	50.83%	0.00%
Mass transfer zone depth, inches	6	8	8	5	8	8	4	4	3.0	3.8
Reference	Soelberg 2014a	Soelberg 2014b		Soelberg 2015	Soelberg 2016		Soelberg 2018		Soelberg 2019	---
					[iodine data less data 26sep19.xlsx]2019 summary short					